Article:
Dorsman, I.R., Derry, M.J., Cunningham, V.J. et al. (3 more authors) (2021) Tuning the vesicle-to-worm transition for thermoresponsive block copolymer vesicles prepared via polymerisation-induced self-assembly. Polymer Chemistry, 12 (9). pp. 1224-1235. ISSN 1759-9954

https://doi.org/10.1039/d0py01713b

Supporting Information for *Polymer Chemistry* article:

Tuning the Vesicle-to-Worm Transition for Thermoresponsive Block Copolymer Vesicles Prepared via Polymerisation-Induced Self-Assembly

Isabella R. Dorsman, Matthew J. Derry, Victoria J. Cunningham, Steven L. Brown, Clive N. Williams and Steven P. Armes*

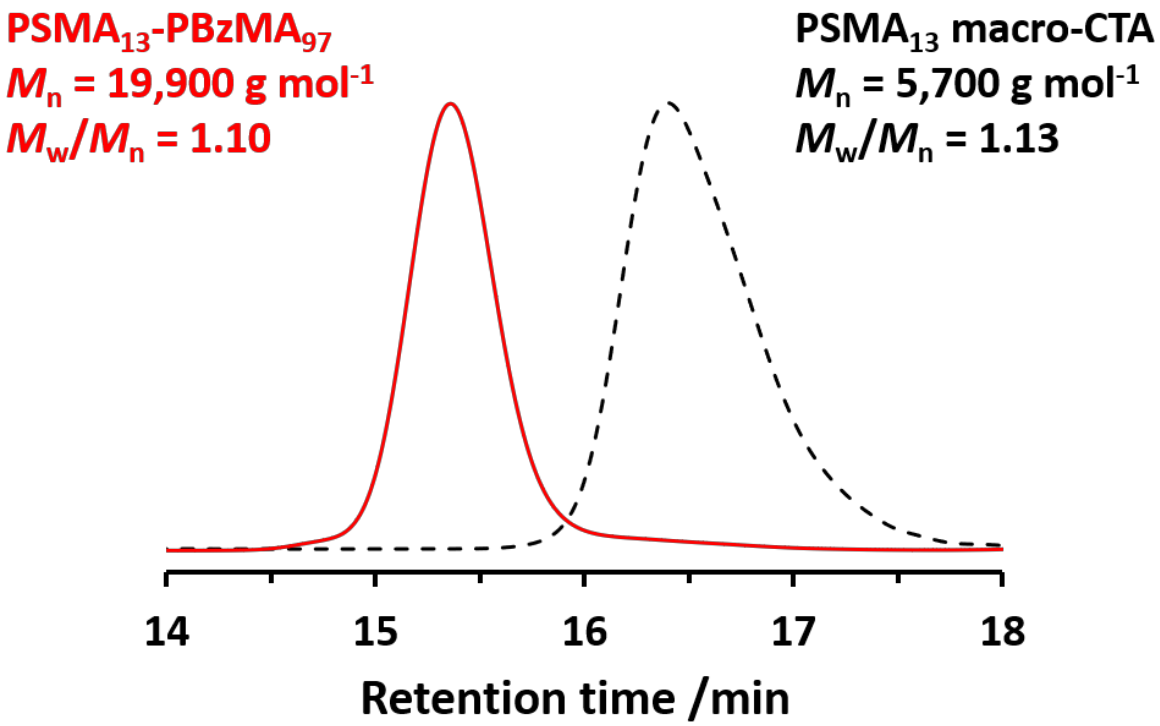

Fig. S1 THF GPC traces recorded for $PSMA_{13}$-$PBzMA_{97}$ diblock copolymer chains and the corresponding $PSMA_{13}$ macro-CTA precursor.

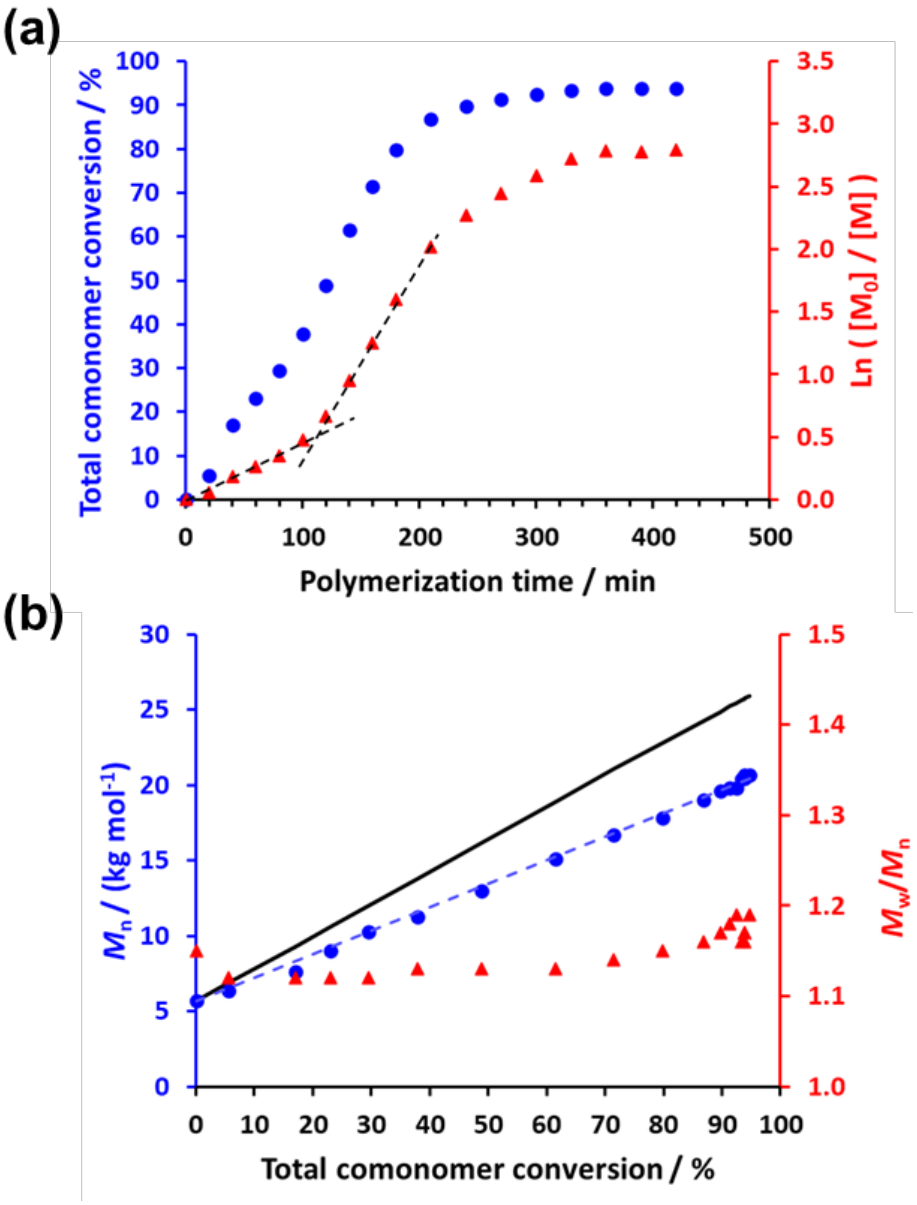

Fig. S2 (a) Overall comonomer conversion vs. time curve (blue circles) and corresponding $\ln([M]_0/[M])$ *vs.* time (red triangles) plot. (b) Evolution in M_n (blue circles) and M_w/M_n (red triangles) with comonomer conversion during the synthesis of $PSMA_{14}$-P(0.5BzMA-*stat*-0.5BuMA)$_{130}$ nanoparticles via RAFT dispersion copolymerization of BzMA with BuMA at 90 °C when targeting 10% w/w solids in mineral oil. The theoretical M_n *vs.* overall comonomer conversion relationship is indicated by the black solid line for this series, with the difference being attributed to the GPC calibration error incurred by using poly(methyl methacrylate) standards.

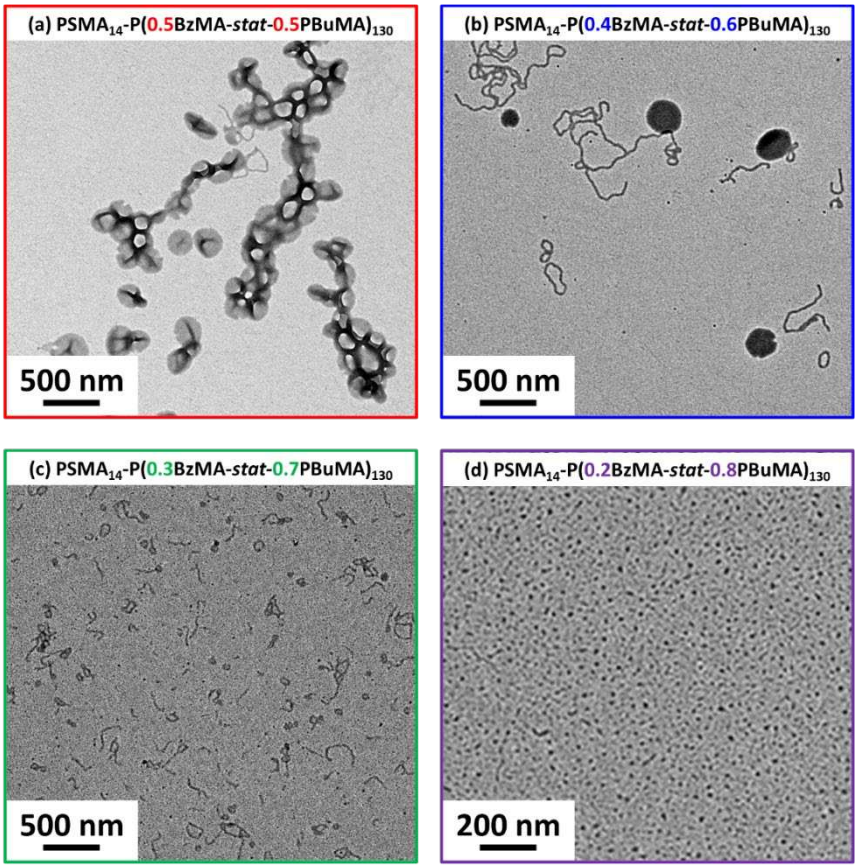

Fig. S3 Representative TEM images at 20 °C for (a) $PSMA_{14}$-P(0.5BzMA-stat-0.5BuMA)$_{130}$ vesicles (and a few worms), (b) $PSMA_{14}$-P(0.4BzMA-stat-0.6BuMA)$_{130}$ vesicles and worms, (c) $PSMA_{14}$-P(0.3BzMA-stat-0.7BuMA)$_{130}$ worms and (d) $PSMA_{14}$-P(0.8BzMA-stat-0.2BuMA)$_{130}$ spheres.

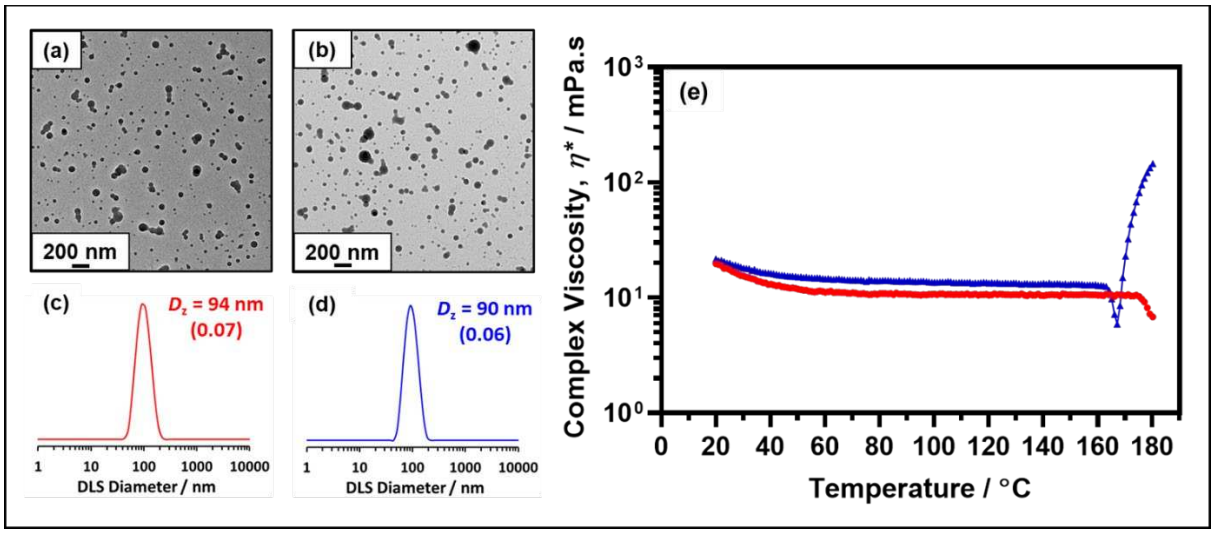

Fig. S4 Representative TEM images at 20 °C for (a) block copolymer vesicles with target composition $PSMA_{14}$-$PBzMA_{130}$ and (b) block copolymer vesicles with target composition $PSMA_{14}$-$PBzMA_{125}$. Intensity-average particle diameter distribution obtained by DLS for a 0.10% w/w dispersion of (c) $PSMA_{14}$-$PBzMA_{130}$ vesicles and (d) $PSMA_{14}$-$PBzMA_{125}$ vesicles. (e) Temperature dependence of the complex viscosity (η^*) observed for $PSMA_{14}$-$PBzMA_{130}$ nanoparticles (red circles) and $PSMA_{14}$-$PBzMA_{130}$ nanoparticles (blue triangles) on heating from 20 °C to 180 °C at 2°C min^{-1}. Data were obtained at 1.0 % strain using an angular frequency of 10 rad s^{-1}.

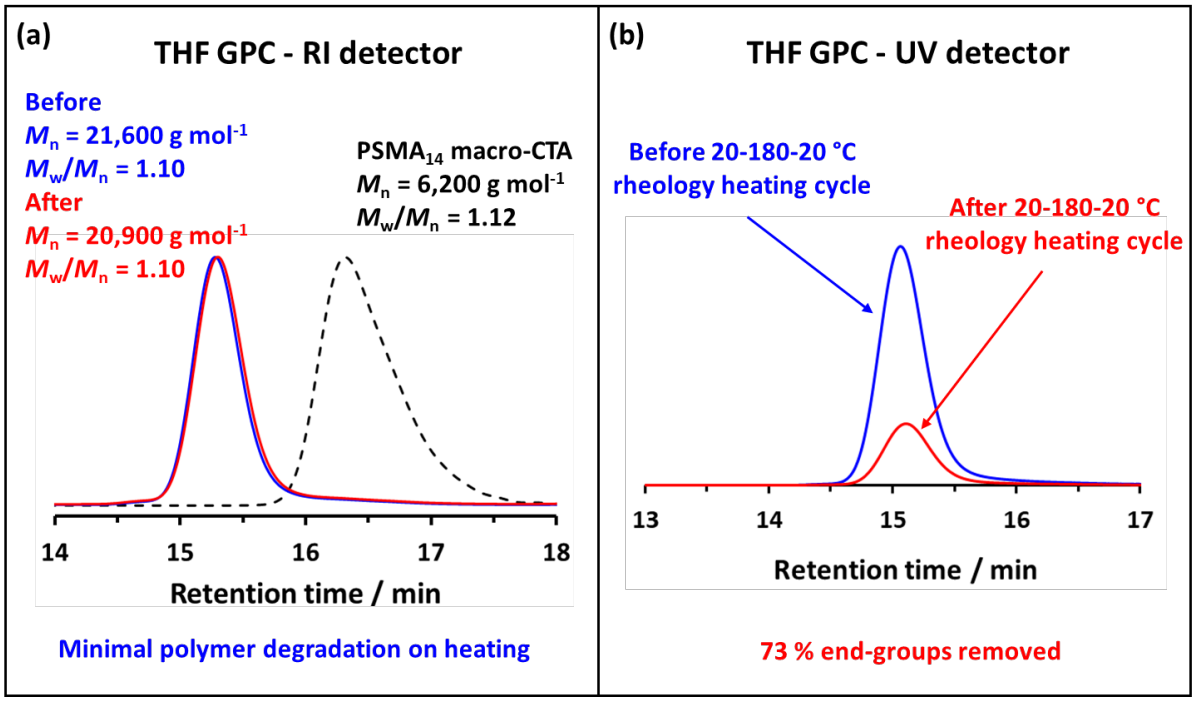

Fig. S5 THF GPC analysis of PSMA$_{14}$-P(0.5BzMA-*stat*-0.5BuMA)$_{130}$ chains before (blue traces) and after (red traces) subjecting a 10% w/w dispersion of such diblock copolymer nano-objects in mineral oil to a 20-180-20 °C thermal cycle in a rheology experiment. (a) Refractive index (RI) detector with the PSMA$_{14}$ macro-CTA included as a reference. (b) UV detector set at λ = 302 nm.

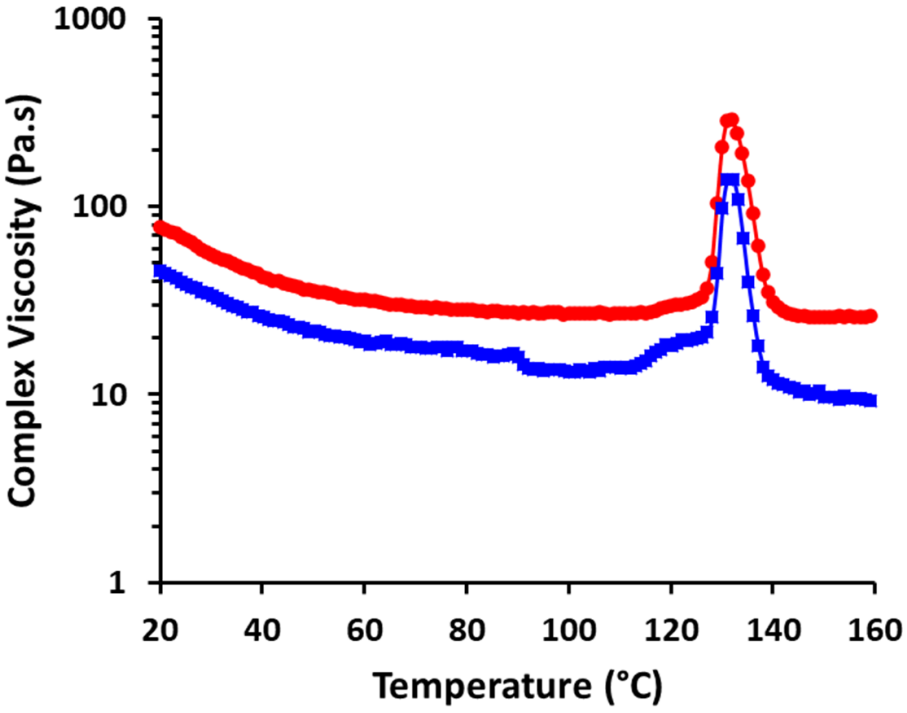

Fig. S6 Temperature dependence of the complex viscosity (η*) observed for PSMA$_{14}$-P(0.5BzMA-*stat*-0.5BuMA)$_{130}$ nano-objects on heating from 20 °C to 160 °C. Red circles indicate data obtained for an 'as-synthesized' 10% w/w dispersion of PSMA$_{14}$-P(0.5BzMA-*stat*-0.5BuMA)$_{130}$ nano-objects in mineral oil, (92% BuMA conversion, as determined by ^{1}H NMR spectroscopy). Blue squares indicate data obtained for an equivalent 10% w/w dispersion of PSMA$_{14}$-P(0.5BzMA-*stat*-0.5BuMA)$_{130}$ with post-polymerization addition of the

equivalent of 8% residual BuMA (thus doubling the mass of residual BuMA comonomer that is present). Clearly, the addition of BuMA comonomer has minimal effect on the observed behavior.

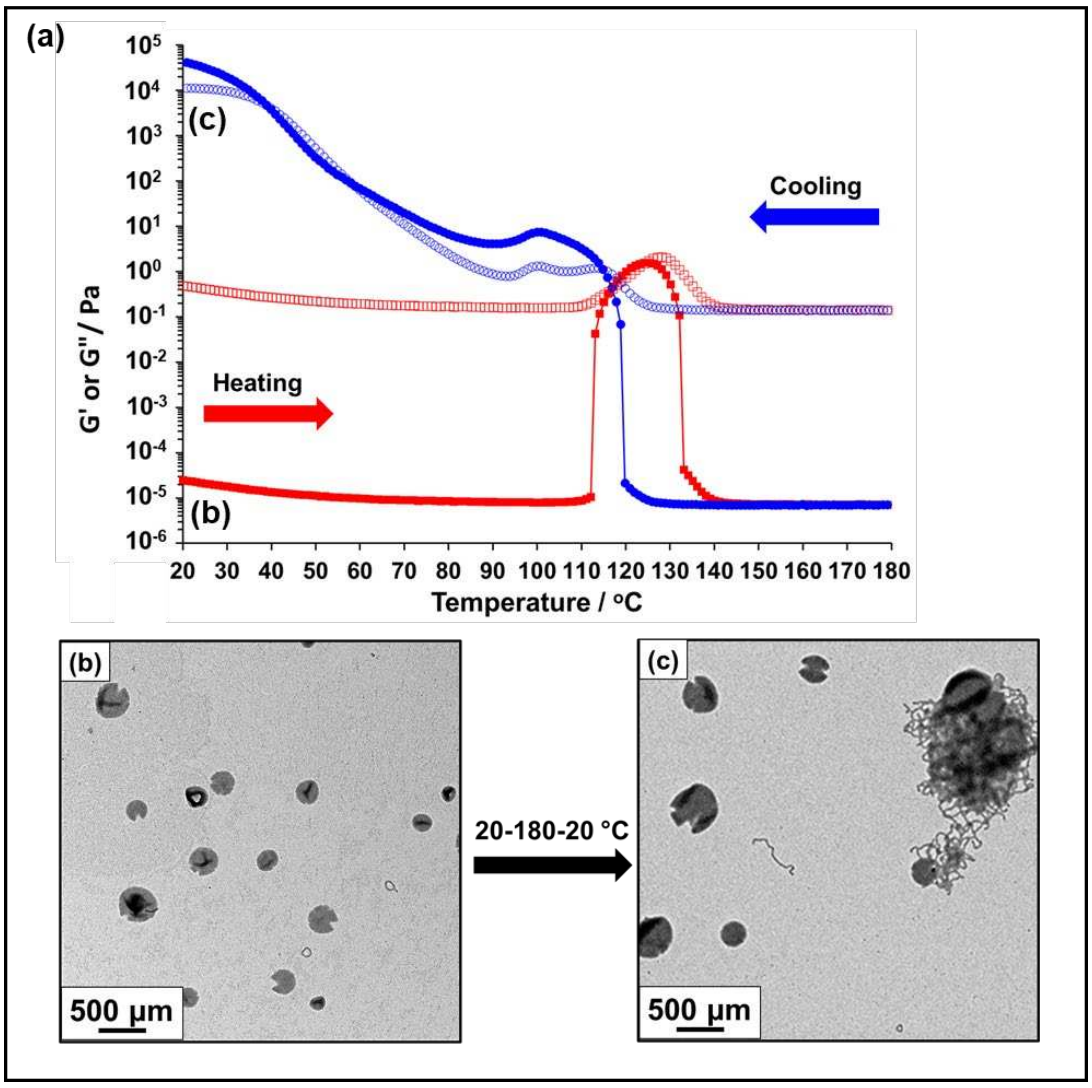

Fig. S7 (a) Temperature dependence of the storage modulus (*G'*, red filled squares) and loss modulus (*G"*, red empty squares) observed for a 10% w/w dispersion of $PSMA_{14}$-P(0.5BzMA-*stat*-0.5BuMA)$_{130}$ nano-objects in mineral oil when heating from 20 to 180 °C at 2 °C min^{-1}. The storage and loss moduli were also recorded on cooling the sample back down to 20 °C at 2 °C min^{-1} (*G'* = blue filled circles and *G"* = blue empty circles). This experiment was conducted at 1.0% strain and an angular frequency of 10 rad s^{-1}. Representative TEM images recorded after drying 0.10% w/w dispersions of $PSMA_{14}$-P(0.5BzMA-*stat*-0.5BuMA)$_{130}$ nano-objects at 20 °C (b) before and (c) after the 20-180-20 °C thermal cycle.

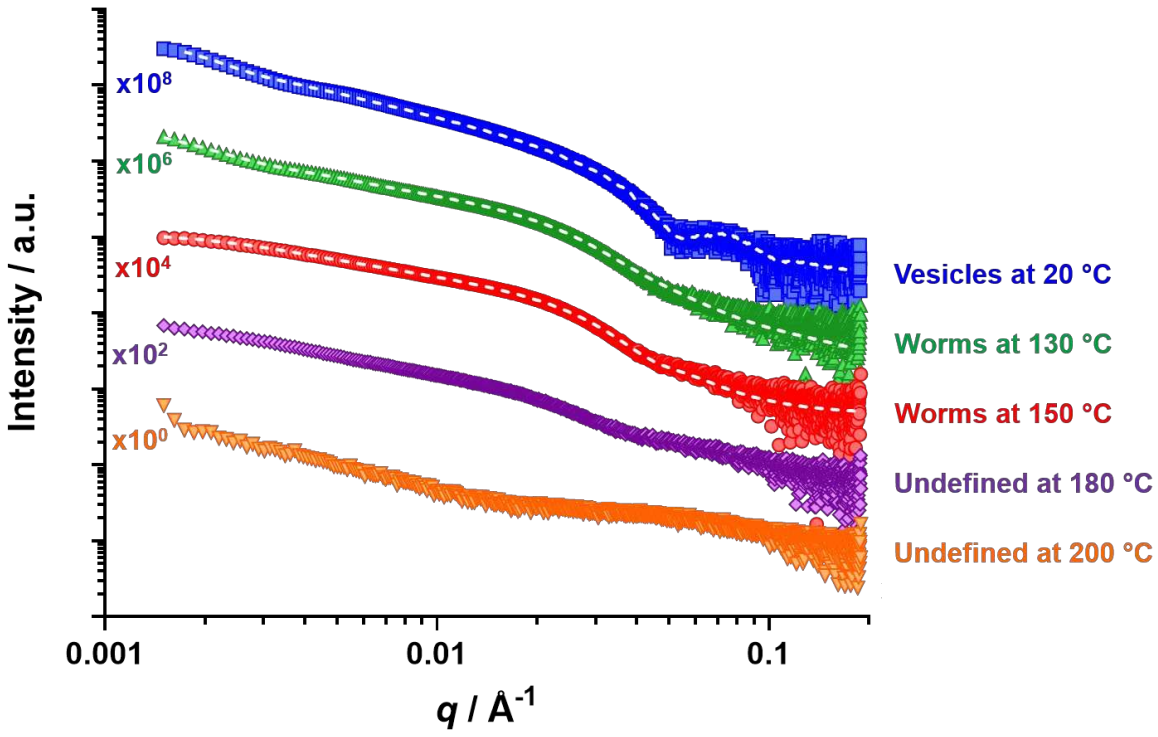

Fig. S8 Representative SAXS patterns recorded for $PSMA_{14}$-P(0.5BzMA-*stat*-0.5BuMA)$_{130}$ nano-objects at 20 °C, 130 °C and 150 °C, with dashed lines indicating the data fits obtained using the relevant scattering model (as shown in Fig. 7). The patterns recorded at 180 °C and 200 °C could not be satisfactorily fitted using any of the scattering models presented herein.